RESEARCH ARTICLE | AUGUST 20 2014

Metamorphic $Ga_{0.76}In_{0.24}As/GaAs_{0.75}Sb_{0.25}$ tunnel junctions grown on GaAs substrates FREE

I. García; J. F. Geisz; R. M. France; J. Kang; S.-H. Wei; M. Ochoa; D. J. Friedman

Journal of Applied Physics 116, 074508 (2014)
https://doi.org/10.1063/1.4892773
CHORUS

Metamorphic $Ga_{0.76}In_{0.24}As/GaAs_{0.75}Sb_{0.25}$ tunnel junctions grown on GaAs substrates

I. García,[1,2] J. F. Geisz,[1] R. M. France,[1] J. Kang,[1] S.-H. Wei,[1] M. Ochoa,[1,2] and D. J. Friedman[1]
[1]*National Renewable Energy Laboratory, Golden, Colorado 80401, USA*
[2]*Instituto de Energía Solar, Universidad Politécnica de Madrid, Avda. Complutense s/n, 28040 Madrid, Spain*

(Received 19 June 2014; accepted 25 July 2014; published online 20 August 2014)

Lattice-matched and pseudomorphic tunnel junctions have been developed in the past for application in a variety of semiconductor devices, including heterojunction bipolar transistors, vertical cavity surface-emitting lasers, and multijunction solar cells. However, *metamorphic* tunnel junctions have received little attention. In 4-junction $Ga_{0.51}In_{0.49}P/GaAs/Ga_{0.76}In_{0.24}As/Ga_{0.47}In_{0.53}As$ inverted-metamorphic solar cells (4J-IMM), a metamorphic tunnel junction is required to series connect the 3rd and 4th junctions. We present a tunnel junction based on a metamorphic $Ga_{0.76}In_{0.24}As/GaAs_{0.75}Sb_{0.25}$ structure for this purpose. This tunnel junction is grown on a metamorphic $Ga_{0.76}In_{0.24}As$ template on a GaAs substrate. The band offsets in the resulting type-II heterojunction are calculated using the first-principles density functional method to estimate the tunneling barrier height and assess the performance of this tunnel junction against other material systems and compositions. The effect of the metamorphic growth on the performance of the tunnel junctions is analyzed using a set of metamorphic templates with varied surface roughness and threading dislocation density. Although the metamorphic template does influence the tunnel junction performance, all tunnel junctions measured have a peak current density over 200 A/cm^2. The tunnel junction on the best template has a peak current density over 1500 A/cm^2 and a voltage drop at 15 A/cm^2 (corresponding to operation at 1000 suns) lower than 10 mV, which results in a nearly lossless series connection of the 4th junction in the 4J-IMM structure.
 [http://dx.doi.org/10.1063/1.4892773]

I. INTRODUCTION

Tunnel junctions are an essential component of many electronic devices including heterojunction bipolar transistors (HBTs), vertical cavity surface-emitting lasers (VCSELS), and multijunction solar cells. Their usual role is to be a low resistance interconnection between different parts of the device semiconductor structure. Therefore, they are primarily required to have a high peak current and a very low specific resistance. In some optoelectronic device applications, the tunnel junction structure is also required to be transparent to certain photon wavelength ranges. For example, in VCSELS[1] the tunnel junction must be transparent to the narrow lasing wavelength range, and in multijunction solar cells,[2] the absorption must be minimized in the range of photon wavelengths that must be transmitted to the subcells underneath the tunnel junction. 4-junction inverted-metamorphic solar cells (4J-IMM) are composed of two upper junctions, GaInP and GaAs, lattice matched to a GaAs substrate, followed by two metamorphic GaInAs junctions with 1 eV and 0.7 eV bandgaps.[3,4] This 4J-IMM solar cell in based on the 3J-IMM GaInP/GaAs/GaInAs structure developed previously,[5] where the GaInAs bottom cell has ~2% lattice mismatch to the GaAs substrate, and is accessed by using a compositionally graded buffer (CGB) to transition the lattice constant between subcells. The 0.7 eV GaInAs material required for the 4th junction is attained by further expanding the lattice to a total mismatch of ~4% to the GaAs substrate, and high-quality single junction subcells with this bandgap have been demonstrated.[6] Efficiencies over 48% under concentration are expected for the 4J-IMM in the near term. However, integration of this new subcell requires a metamorphic tunnel junction between the 3rd and 4th subcells, as shown in Figure 1. In this structure, the tunnel junction that interconnects the 1st to the 2nd subcell is grown lattice matched to the GaAs substrate. The third subcell is metamorphic, but the tunnel junction interconnect between the 2nd and 3rd subcells can be lattice-matched to the GaAs substrate if placed before the compositionally graded buffer. The third tunnel junction, which connects the 1 eV (3rd) and 0.7 eV (4th) subcells, must be metamorphic, and can be grown with the same lattice constant as the metamorphic 1 eV $Ga_{0.76}In_{0.24}As$ material. Little research has been performed on metamorphic tunnel junctions. As compared to the lattice-matched and pseudomorphic cases, the growth of semiconductor structures and, in particular, of tunnel junctions, on metamorphic templates may be complicated by factors including surface roughness, local microscale strain and composition variations and threading dislocations, which are typical of these metamorphic layers[7,8] and can affect the growth and performance of the devices grown on these templates. Concerning optical absorption, the 3rd junction in the 4J-IMM is usually made optically thick, so any material with the bandgap of $Ga_{0.76}In_{0.24}As$ (~1 eV) or higher allows this tunnel junction to meet the requirement of transparency.

Previous research on tunnel junctions grown either pseudomorphic or lattice-matched to InP has used both GaInAs/

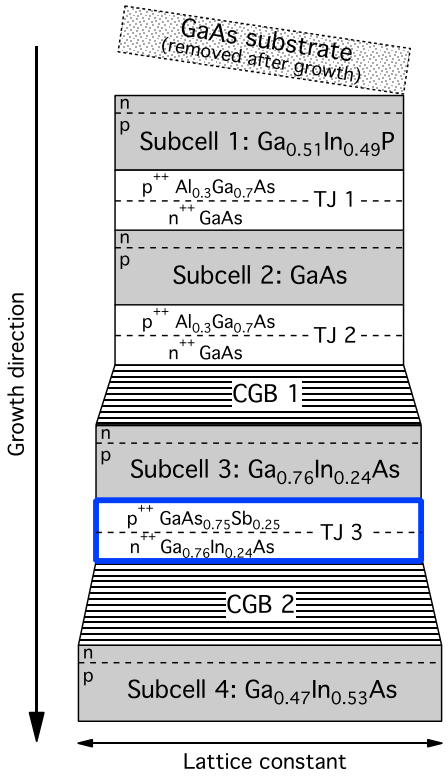

FIG. 1. Structure of the 4J-IMM cell, including the metamorphic $Ga_{0.76}In_{0.24}As/GaAs_{0.75}Sb_{0.25}$ tunnel junction (TJ3) presented in this work. The horizontal dimension of the drawing schematically illustrates the lattice constant of the materials. The figure is not to scale.

GaInAs and GaInAs/GaAsSb material combinations. $Ga_{0.47}In_{0.53}As/Ga_{0.47}In_{0.53}As$ tunnel junctions grown by MBE or MOMBE using beryllium as p-type dopant have shown very high peak current densities over 10 kA/cm^2.[9,10] However, in a MOVPE environment, zinc and carbon are the most frequent p-type dopants used. It is normally advisable to steer away from zinc for tunnel junctions, in order to minimize dopant diffusion and tunnel junction performance degradation during the growth of the next layers in the structure. P-type doping of GaInAs using carbon involves dealing with issues such as the amphoteric behavior of carbon which, together with a lower binding energy for C-In than for C-As, gives rise to preferential incorporation of C in In sites leading to n-type doping, an effect that is made stronger as the In composition increases.[11] Besides, using CBr_4 and CCl_4 halides to dope GaInAs in MOVPE was found to strongly affect the growth rate and surface morphology due to fast etching of In by these halides. However, heavy carbon doping levels have been attained in GaInAs for In compositions <0.5 at low temperatures by appropriately adjusting the constituent flows to compensate for the In etch.[12]

The alternative option explored in this work for our metamorphic tunnel junction is using GaAsSb. Its growth by MOVPE poses another set of complications, as will be explained later, but very high carbon doping levels can easily be attained in this material using CBr_4 or CCl_4.[13,14] Moreover, another benefit of using this material in a GaInAs/GaAsSb tunnel junction is the type-II band alignment that these structures exhibit, which is reported to facilitate the tunneling of carriers via a lower tunneling barrier.[15] Pseudomorphic GaAsSb/GaInAs structures were developed in the past for InP-based tandem solar cells,[16] achieving extremely high peak current densities over 19 kA/cm^2. State-of-the-art $Ga_{0.47}In_{0.53}As/GaAs_{0.51}Sb_{0.49}$ tunnel junctions lattice-matched to InP substrates exhibit peak tunneling currents over 572 kA/cm^2.[17] Pseudomorphic $GaAs_{0.88}Sb_{0.12}/Ga_{0.84}In_{0.16}As$ tunnel junctions grown on GaAs substrates were developed for VCSELs structures working at lasing wavelengths as high as 1.1 μm, demonstrating the advantage of using a type-II band alignment.[15]

In this work, we present the development of a high performance metamorphic $Ga_{0.76}In_{0.24}As/GaAs_{0.75}Sb_{0.25}$ tunnel junction grown on GaAs. The band offsets in this system, which determine the tunneling probability, are calculated and used to compare its performance to existing pseudomorphic or lattice-matched tunnel junctions. The effect of the metamorphic template on the tunnel junction is also studied.

II. CALCULATION OF THE BAND OFFSETS IN THE GaInAs/GaAsSb SYSTEM.

The tunneling probability is exponentially sensitive to the actual band offsets in the type-II band diagram of the GaInAs/GaAsSb structure.[15] The band offsets depend on the compositions of GaAsSb and GaInAs used in the structure. In Refs. 18, and 19 compilations of calculated and measured band offsets for a set of material systems are presented. In view of the significant dispersion in the data obtained, the authors in Ref. 19 provide a set of "recommended" offsets, as a result of the comparative analysis of the data. The GaAsSb/GaInAs system has received relatively little study and for the composition used for the metamorphic tunnel junction presented here ($Ga_{0.76}In_{0.24}As/GaAs_{0.75}Sb_{0.25}$), no measured or calculated data is available. In order to extend the data available in the literature and estimate the actual band offsets in this system as an input for the subsequent analysis we carry out in this paper, we have computed the natural band offsets in the GaInAs/GaAsSb structure for a range of material compositions using first-principles density functional method. To model the fully disordered random alloys, we used large special quasirandom structures (SQS's[20,21]) consisting of 512 atoms in a cubic supercell. Local density approximation (LDA[22]) was employed to calculate the valence-band offsets. Spin-orbit splitting of the valence bands was also considered. The valence-band offsets (referenced to that of GaAs) were obtained by first calculating the band offset between the SQS and a strained cubic GaAs whose lattice constant matches that of the SQS. Core-levels of the common cations (or anions) in the SQS/GaAs heterostructures are used as references to determine the band offset.[23] Then, the valence-band energy of the strained GaAs in the model system was shifted back to the value at the equilibrium lattice constant using the absolute volume deformation potential[24] of GaAs. To correct the well-known LDA bandgap underestimation, we performed hybrid DFT calculations using the screened Heyd-Scuseria-Ernzerhof (HSE[25]) hybrid density functional, as implemented in the VASP package.[26] The bowing parameters of the bandgaps were calculated to be $b = 1.15$ eV and 0.52 eV for GaAsSb and

GaInAs, respectively. The HSE bowing parameters that were obtained using the large SQS supercells agree well with the experimental values ($b_{GaAsSb} = 1.2$ eV (Refs. 27–29) and $b_{GaInAs} = 0.48$ eV (Ref. 19)). The conduction-band offsets were obtained by using the calculated valence-band offsets and the bowing parameters. In the DFT calculations, we used experimental lattice constants at room temperature and fully relaxed the atomic coordinates of the SQS supercells.

The results are shown in Figure 2. The fact that the GaInAs/GaAsSb structure is type-II is made apparent in this graph. As can be observed, for materials lattice matched to InP ($Ga_{0.47}In_{0.53}As/GaAs_{0.51}Sb_{0.49}$) the band discontinuities are larger than for compositions of materials closer to the GaAs lattice constant. Since the tunneling barrier height and width depends on these discontinuities,[15] the tunneling probability enhancement provided by the type-II alignment should be less pronounced in our tunnel junction. This obviously affects the tunnel junction performance, as will be shown in Sec. IV.

III. MOVPE GROWTH OF THE GaInAs/GaAsSb TUNNEL JUNCTIONS

The tunnel junctions developed in this work were grown by MOVPE in a custom-built vertical, atmospheric pressure reactor. Details of the tunnel junction growth parameters are summarized in Table I. The MOVPE growth of this metamorphic tunnel junction poses some challenges. The growth

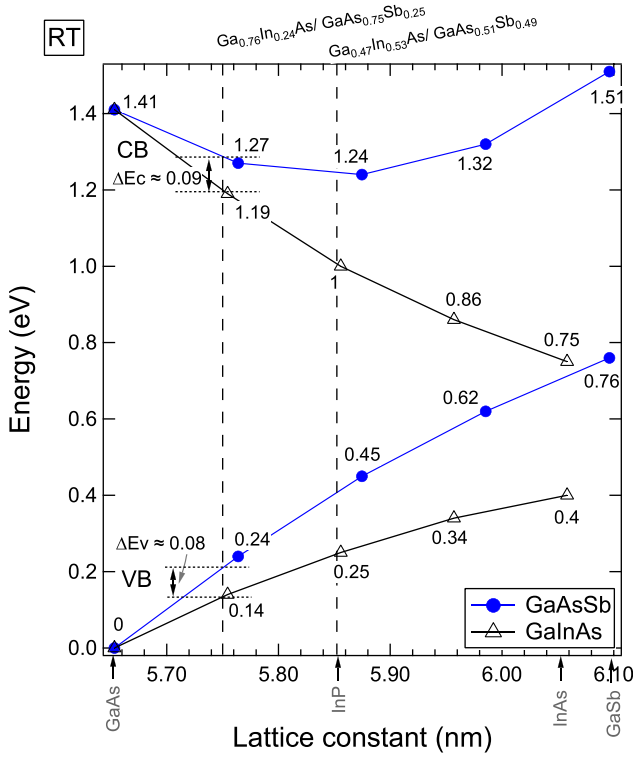

FIG. 2. Band offsets in heterostructures comprising GaInAs and GaAsSb materials, as calculated using the first-principles density functional method at room temperature (see text for extended description). The valence and conduction band offsets for the $Ga_{0.76}In_{0.24}As/GaAs_{0.75}Sb_{0.25}$ structure are indicated.

TABLE I. Reactor characteristics and optimized growth parameters used for GaAsSb and GaInAs in the tunnel junctions presented in this work. All ratios indicated correspond to the gas-phase.

Reactor	Vertical, atmospheric pressure, RF heater					
Precursors	TMGa, TESb, TMIn, AsH_3, PH_3 H_2Se, Si_2H_4, CCl_4					
	T_g [°C]	P [mbar]	GR [μm/h]	V/III	Sb/V	Sb/III
GaAsSb	550	~815	1.5	1.2	0.26	0.31
GaInAs	550	~815	4.5	15	…	…

of the metastable GaAsSb compound presents a complicated chemistry with very narrow growth condition windows to attain the required structural quality, due mainly to the low volatility of Sb and the large miscibility gap of GaAsSb.[30] The particular precursors used also play a role in the growth dynamics and, in combination with the growth conditions, determine the quality of the material.[30,31] However good structural and electronic quality GaAsSb grown by MOVPE, mainly lattice matched to InP, has been presented in the past.[32] The growth parameters shown in Table I were used in this work for the metamorphic $GaAs_{0.75}Sb_{0.25}$ layers. We have confirmed the previous observations by other authors that the V/III ratio must be ~1 to achieve the highest Sb incorporation efficiency.[33,34] At the growth conditions used (Table I) we observed a linear dependence of the GaAsSb composition with the AsH_3/TESb ratio. Sb tends to segregate and not to incorporate before a certain surface concentration is reached, as observed by RDS measurements.[34] Therefore, prior to growth of the GaAsSb anode in our tunnel junctions, the surface is soaked with Sb and As for 6 s, in order to prompt the Sb incorporation as soon as TMGa is introduced into the reactor. Failure to do so was observed to produce GaAsSb layers with unexpectedly low Sb content.

Extrinsic carbon doping using CCl_4 or CBr_4 complicates the MOVPE growth of GaAsSb by altering the net incorporation of constituents and, consequently, changing the composition of the material and the growth rate.[13,14] Higher temperatures led to lower growth rates and higher Sb incorporation, similarly as found for CBr_4 in Ref. 14. Yet for the low growth temperature used for the optimized material in this work (see Table I), the effect of CCl_4 was found to be still significant. Nevertheless, changing the gas phase concentration of the constituents we could easily compensate for the deviation of the composition caused by the CCl_4. Thus, the calibration of the GaAsSb material growth must be done using the CCl_4 flow required to attain the objective doping concentration.

Strain also influences the growth of GaAsSb.[31,35] In the metamorphic structure presented here, the tunnel junctions are designed to be strain-free by carefully designing the compositionally graded buffer. However, crosshatch roughness and micron-scale small composition variations are present on the surface due to the effect of the strain fields induced by the misfit dislocations introduced during the relaxation of the metamorphic buffer structures.[7,8,36] The interaction of this

roughness and the composition variations with the already complicated growth chemistry must be considered when assessing the quality of the material and structures grown, and may have an influence on the dependence of the tunnel junctions on the roughness of the metamorphic templates shown later.

The tunnel junction semiconductor structure under study is grown on GaAs substrates with a metamorphic buffer to access the lattice constant of $Ga_{0.76}In_{0.24}As$ (see Figure 1). Carbon and selenium are used as p- and n-type dopants, respectively. The anode and cathode were chosen to be relatively thick (50 nm) in order to limit the effect of the surrounding layers on the band bending whose influence on the performance of the tunnel junction is difficult to predict. Since the absorption of light in this tunnel junction is expected to be negligible, as noted in the introduction, using a relatively thick tunnel junction was not considered a problem for the overall conclusions about the performance analysis presented here. Both the substrate and the metamorphic buffer are chemically etched before processing the devices. The inset of Figure 3 shows the resulting structure of the tunnel junction devices.

These structures were then processed into 250 × 250 μm tunnel junction devices, using standard photolithographic techniques and gold electroplating. An IV curve tracer was used to obtain the JV curves of these tunnel junctions using the four-point probe technique. In Figure 3, the JV curves of $Ga_{0.76}In_{0.24}As/GaAs_{0.75}Sb_{0.25}$ tunnel junctions with different dopings in the $Ga_{0.76}In_{0.24}As$ cathode are shown. The JV curves show an increasing peak current density with the doping level in the cathode. Peak current densities over 1500 A/cm^2 are obtained for the highest doping levels used. The relatively high specific series resistance exhibited by these tunnel junction devices is limited by the contact resistance of the electroplated gold metal contacts used, so the value shown in the graph can be considered as an upper limit of the actual specific series resistance of the tunnel junction semiconductor structure. Nonetheless, as long as the application of this tunnel junction to the 4J solar cell is concerned, the voltage drop at a current density of 14 A/cm^2, corresponding to an operating concentration of 1000 suns, is below 10 mV. Therefore, these tunnel junctions are suitable for their use as a 3rd tunnel junction in the 4J-IMM structure (Figure 1).

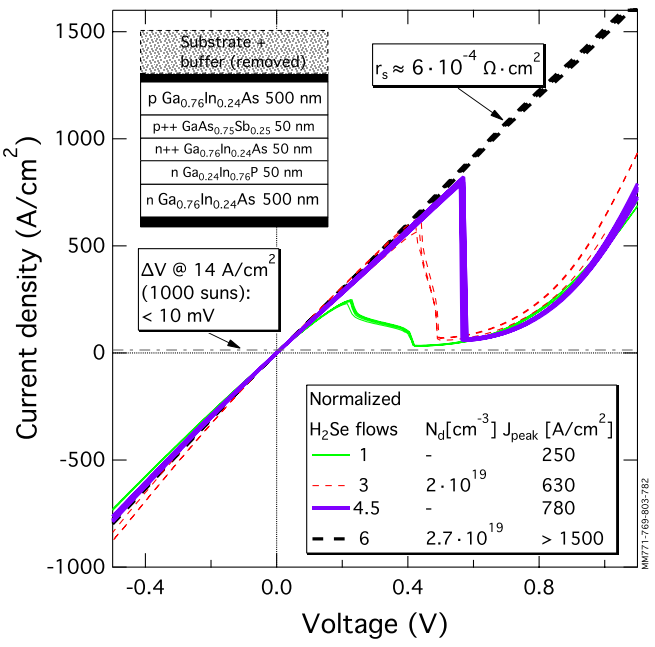

FIG. 3. J-V curves of the tunnel junctions developed, for different normalized H_2Se flows used in the cathode of the tunnel junction. The J-V curves of several identical devices are shown for each case. When available, the GaInAs cathode Hall doping levels measured are indicated. The doping level in the GaAsSb anode is 5×10^{19} cm^{-3} in all cases. The inset shows the tunnel junction structures used in this study. Note that the substrate and metamorphic buffer structure are removed in the tunnel junction devices fabricated. The diodes fabricated are 250 × 250 μm square shaped. The specific series resistance of the tunnel junction devices in the ohmic region indicated is limited by the metal-semiconductor contact resistance.

IV. PERFORMANCE ASSESSMENT OF THE TUNNEL JUNCTION

The performance of these tunnel junctions was further assessed by comparison with other previous pseudomorphic or lattice-matched tunnel junction structures, using the reduced doping level and the tunneling barrier height as the parameters, similar to Ref. 17. The reduced doping level, used commonly for tunnel junction analysis, is defined as the ratio of the product to the sum of the doping levels in the cathode and anode of the tunnel junction ($N^* = Nd \cdot Na/(Nd + Na)$). The difference between the conduction band of the cathode and the valence band of the anode can be used as a quantitative proxy of the actual barrier height for tunneling across the junction in the structure.[17] In the $Ga_{0.76}In_{0.24}As/GaAs_{0.75}Sb_{0.25}$ structure, this tunneling barrier height is

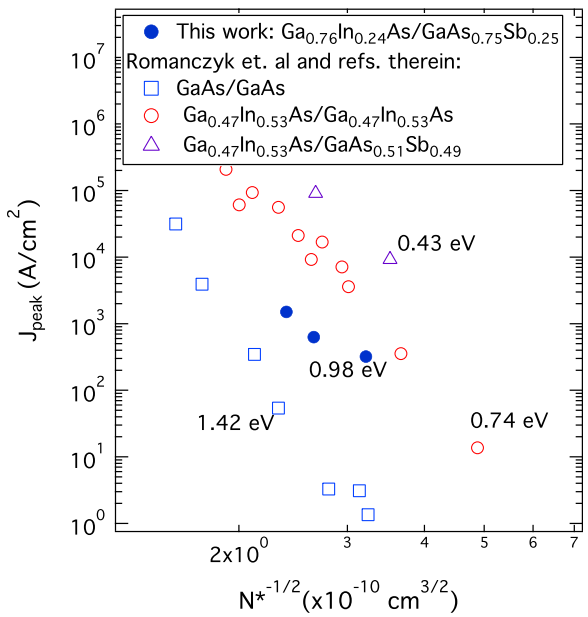

FIG. 4. Peak current density plotted versus the reduced doping density (N*) in the tunnel junction, for different materials and tunneling barrier heights (labels) in the structure, as indicated in the legend. The filled dots correspond to the data obtained for the tunnel junctions presented in this work. The rest of data is obtained from Ref. 17 and references therein. The labels indicate the estimated tunneling barrier height calculated as the difference between the cathode conduction band and the anode valence band.

0.98 eV, as calculated using the band diagram offsets shown in Figure 2. In Figure 4, the peak current density of the $Ga_{0.76}In_{0.24}As/GaAs_{0.75}Sb_{0.25}$ tunnel junctions developed is plotted against the reduced doping density, together with the data corresponding to other material systems compiled in Ref. 17. As can be observed, the performance of the tunnel junction developed in this work fits well in this graph, considering the effect of the tunneling barrier height on the tunneling current. An interesting point to make is the fact that the peak current density of this tunnel junction is lower than in the case of $Ga_{0.47}In_{0.53}As/Ga_{0.47}In_{0.53}As$ lattice matched on InP substrates, even though in this case the band diagram is not type-II. Therefore, as long as the 4J structure is concerned, growing the 3rd tunnel junction after the second metamorphic buffer (see Figure 1), i.e., with a lattice constant of InP, could be advantageous to attain a higher electrical performance. However, this tunnel junction would not be transparent to the light that has to be transmitted to the 4th junction, giving rise to a higher optical absorption and a photocurrent loss in the 4J-IMM. Since the electrical performance of the tunnel junction developed is already very high, as shown in Figure 3, a loss in photocurrent when using a $Ga_{0.47}In_{0.53}As/Ga_{0.47}In_{0.53}As$ tunnel junction would predictably not be compensated for by a better electrical performance.

V. EFFECT OF THE METAMORPHIC TEMPLATE

$Ga_{0.76}In_{0.24}As$ metamorphic templates grown on GaAs substrates, using a GaInP CGB, with relatively low rms roughness and threading dislocation densities (TDDs), around 10 nm and $1 \times 10^6\,cm^{-2}$, respectively, were presented recently.[7] Nevertheless, we wanted to explore if the TDD and roughness from metamorphic buffers influence the performance of the metamorphic tunnel junctions. To test this, we varied the buffer structures using the CGBs presented in Ref. 37, giving rise to different quality $Ga_{0.76}In_{0.24}As$ templates, and subsequently grew identical tunnel junctions on top of these templates. In Figure 5, the peak current density of the resulting tunnel junction devices is plotted against the rms roughness and TDD of the metamorphic templates. As can be observed, lower roughness and TDD produce better performing tunnel junctions. Separating the effects of the roughness and TDD, to ascertain if one or both have any influence, is not straightforward and was not attempted in this work. Possible causes behind this result include composition fluctuations across the tunnel junction area due to the roughness, effect of TDD on dopant diffusion, etc. Concerning the application of these tunnel junctions to 4J-IMM solar cells, for all templates shown in Figure 5, the performance of the tunnel junction is high enough as to serve as a series connection with negligible losses in a multijunction solar cell. However, the influence of the metamorphic template on the performance of the tunnel junction can be important in other cases where the quality of the metamorphic template used is worse or in devices where the attainment of very high tunneling currents is critical.

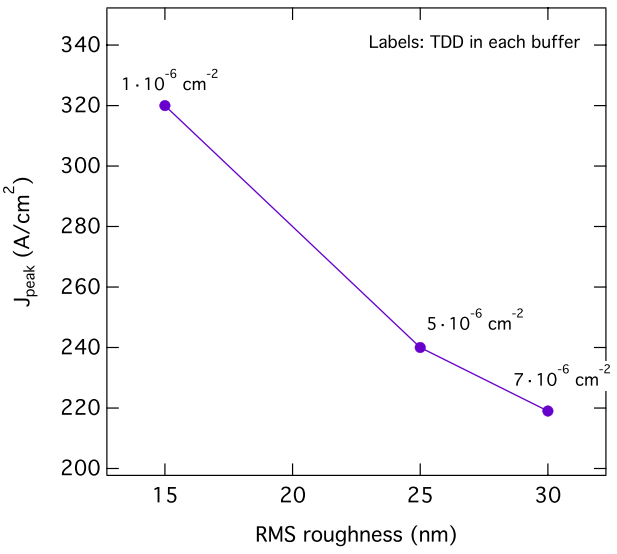

FIG. 5. Peak tunneling current vs. the RMS roughness of the GaInAs templates the tunnel junction is grown on. For each template, a TDD was measured, which is indicated by the labels.

VI. CONCLUSIONS

In conclusion, we have presented a $Ga_{0.76}In_{0.24}As/GaAs_{0.75}Sb_{0.25}$ metamorphic tunnel junction grown on GaAs substrates, assessed its performance against the calculated band discontinuities of the type-II band structure produced at this precise composition and compared its performance to other lattice-matched or pseudomorphic tunnel junctions. A dependency of the TJ performance on the quality of the metamorphic template has been observed. However, the effect is small enough that all templates studied resulted in high quality tunnel junctions for multijunction solar cell applications. With the performance exhibited, this metamorphic tunnel junction enables the series connection of the metamorphic 0.7 eV subcell in 4 J-IMM structures for operation at concentrations higher than 1000 suns without significant losses attributable to the tunnel junction.

ACKNOWLEDGMENTS

The authors thankfully acknowledge the invaluable support by W. Olavarria and M. Young growing and processing the semiconductor devices. I. García holds an IOF grant from the People Programme (Marie Curie Actions) of the European Union's Seventh Framework Programme (FP7/2007-2013) under REA grant agreement No. 299878. This work is supported by the U.S. Department of Energy under Contract No. DE-AC36-08-GO28308 with the National Renewable Energy Laboratory.

[1]M. Ortsiefer, R. Shau, F. Mederer, R. Michalzik, J. Rosskopf, G. Bohm, F. Kohler, C. Lauer, M. Maute, and M.-C. Amann, "High-speed modulation up to 10 Gbit/s with 1.55 μm wavelength InGaAlAs VCSELs," Electron. Lett. **38**(20), 1180–1181 (2002).
[2]I. García, I. Rey-Stolle, and C. Algora, "Performance analysis of AlGaAs/GaAs tunnel junctions for ultra-high concentration photovoltaics," J. Phys. Appl. Phys. **45**(4), 045101 (2012).
[3]D. J. Friedman, J. F. Geisz, A. G. Norman, M. W. Wanlass, and S. R. Kurtz, "0.7-eV GaInAs Junction for a GaInP/GaAs/GaInAs(1eV)/GaInAs(0.7eV) Four-Junction Solar Cell," in *Conference Record of the*

2006 IEEE 4th World Conference on Photovoltaic Energy Conversion (2006), Vol. 1, pp. 598–602.
[4]M. Stan, D. Aiken, B. Cho, A. Cornfeld, V. Ley, P. Patel, P. Sharps, and T. Varghese, "High-efficiency quadruple junction solar cells using OMVPE with inverted metamorphic device structures," J. Cryst. Growth **312**(8), 1370–1374 (2010).
[5]J. F. Geisz, S. Kurtz, M. W. Wanlass, J. S. Ward, A. Duda, D. J. Friedman, J. M. Olson, W. E. McMahon, T. E. Moriarty, and J. T. Kiehl, "High-efficiency GaInP/GaAs/InGaAs triple-junction solar cells grown inverted with a metamorphic bottom junction," Appl. Phys. Lett. **91**(2), 023502 (2007).
[6]R. M. France, I. Garcia, W. E. McMahon, A. G. Norman, J. Simon, J. F. Geisz, D. J. Friedman, and M. J. Romero, "Lattice-mismatched 0.7-eV GaInAs solar cells grown on GaAs using GaInP compositionally graded buffers," IEEE J. Photovolt. **4**(1), 190–195 (2014).
[7]R. M. France, J. F. Geisz, M. A. Steiner, B. To, M. J. Romero, W. J. Olavarria, and R. R. King, "Reduction of crosshatch roughness and threading dislocation density in metamorphic GaInP buffers and GaInAs solar cells," J. Appl. Phys. **111**(10), 103528 (2012).
[8]K. Mukherjee, D. A. Beaton, A. Mascarenhas, M. T. Bulsara, and E. A. Fitzgerald, "Effects of dislocation strain on the epitaxy of lattice-mismatched AlGaInP layers," J. Cryst. Growth **392**, 74–80 (2014).
[9]G. M. Cohen, D. Ritter, and C. Cytermann, "High peak tunnel current density $Ga_{0.47}In_{0.53}As$ Esaki diodes," Electron. Lett. **31**(17), 1511–1512 (1995).
[10]D. Pawlik, M. Barth, P. Thomas, S. Kurinec, S. Mookerjea, D. Mohata, S. Datta, S. Cohen, D. Ritter, and S. Rommel, "Sub-micron InGaAs Esaki diodes with record high peak current density," in *Device Research Conference (DRC), 2010* (2010), pp. 163–164.
[11]H. Ito and T. Ishibashi, "Carbon Incorporation in (AlGa)As, (AlIn)As and (GaIn)As ternary alloys grown by molecular-beam epitaxy," Jpn. J. Appl. Phys. Part 2 **30**(6A), L944–L947 (1991).
[12]S. A. Stockman, A. W. Hanson, and G. E. Stillman, "Growth of carbon-doped p-type $InxGa_{1-x}As$ $(0 < x \leq 0.53)$ by metalorganic chemical vapor deposition," Appl. Phys. Lett. **60**(23), 2903–2905 (1992).
[13]S. P. Watkins, O. J. Pitts, C. Dale, X. G. Xu, M. W. Dvorak, N. Matine, and C. R. Bolognesi, "Heavily carbon-doped GaAsSb grown on InP for HBT applications," J. Cryst. Growth **221**, 59–65 (2000).
[14]O. Ostinelli and C. R. Bolognesi, "Impact of CBr_4, V/III ratio, temperature and AsH_3 concentration on MOVPE growth of GaAsSb:C," J. Cryst. Growth **311**(6), 1508–1514 (2009).
[15]N. Suzuki, T. Anan, H. Hatakeyama, and M. Tsuji, "Low resistance tunnel junctions with type-II heterostructures," Appl. Phys. Lett. **88**(23), 231103 (2006).
[16]J. C. Zolper, J. F. Klem, T. A. Plut, and C. P. Tigges, "GaAsSb-based heterojunction tunnel diodes for tandem solar cell interconnects," in *IEEE Photovoltaic Specialists Conference—1994, 1994 IEEE First World Conference on Photovoltaic Energy Conversion, 1994., Conference Record of the Twenty Fourth* (1994), vol. 2, pp. 1843–1846.
[17]B. Romanczyk, P. Thomas, D. Pawlik, S. L. Rommel, W.-Y. Loh, M. H. Wong, K. Majumdar, W.-E. Wang, and P. D. Kirsch, "Benchmarking current density in staggered gap $In_{0.53}Ga_{0.47}As/GaAs_{0.5}Sb_{0.5}$ heterojunction Esaki tunnel diodes," Appl. Phys. Lett. **102**(21), 213504 (2013).
[18]E. Yu, J. Mccaldin, and T. Mcgill, "Band offsets in semiconductor heterojunctions," Solid State Phys. Adv. Res. Appl. **46**, 1–146 (1992).
[19]I. Vurgaftman, J. R. Meyer, and L. R. Ram-Mohan, "Band parameters for III–V compound semiconductors and their alloys," J. Appl. Phys. **89**(11), 5815–5875 (2001).
[20]A. Zunger, S.-H. Wei, L. G. Ferreira, and J. E. Bernard, "Special quasirandom structures," Phys. Rev. Lett. **65**(3), 353–356 (1990).
[21]S.-H. Wei, L. G. Ferreira, J. E. Bernard, and A. Zunger, "Electronic properties of random alloys: Special quasirandom structures," Phys. Rev. B **42**(15), 9622–9649 (1990).
[22]D. M. Ceperley and B. J. Alder, "Ground state of the electron gas by a stochastic method," Phys. Rev. Lett. **45**(7), 566–569 (1980).
[23]S.-H. Wei and A. Zunger, "Role of d orbitals in valence-band offsets of common-anion semiconductors," Phys. Rev. Lett. **59**(1), 144–147 (1987).
[24]Y.-H. Li, X. G. Gong, and S.-H. Wei, "Ab initio all-electron calculation of absolute volume deformation potentials of IV-IV, III-V, and II-VI semiconductors: The chemical trends," Phys. Rev. B **73**(24), 245206 (2006).
[25]J. Heyd, G. E. Scuseria, and M. Ernzerhof, "Hybrid functionals based on a screened Coulomb potential," J. Chem. Phys. **118**(18), 8207–8215 (2003).
[26]G. Kresse and J. Furthmüller, "Efficient iterative schemes for ab initio total-energy calculations using a plane-wave basis set," Phys. Rev. B **54**(16), 11169–11186 (1996).
[27]R. E. Nahory, M. A. Pollack, J. C. DeWinter, and K. M. Williams, "Growth and properties of liquid phase epitaxial $GaAs_{1-x}Sb_x$," J. Appl. Phys. **48**(4), 1607–1614 (1977).
[28]J. Klem, D. Huang, H. Morkoç, Y. E. Ihm, and N. Otsuka, "Molecular beam epitaxial growth and low temperature optical characterization of $GaAs_{0.5}Sb_{0.5}$ on InP," Appl. Phys. Lett. **50**(19), 1364–1366 (1987).
[29]R. M. Cohen, M. J. Cherng, R. E. Benner, and G. B. Stringfellow, "Raman and photoluminescence spectra of $GaAs_{1-x}Sb_x$," J. Appl. Phys. **57**(10), 4817–4819 (1985).
[30]G. B. Stringfellow, *Organometallic Vapor-Phase Epitaxy: Theory and Practice* (Academic Press, 1999).
[31]T. F. Kuech, A. A. Khandekar, M. Rathi, L. J. Mawst, J. Y. T. Huang, X. Song, S. E. Babcock, J. R. Meyer, and I. Vurgaftman, "MOVPE growth of antimonide-containing alloy materials for long wavelength applications," J. Cryst. Growth **310**(23), 4826–4830 (2008).
[32]M. J. Cherng, G. G. Stringfellow, and R. M. Cohen, "Organometallic vapor phase epitaxial growth of $GaAs_{0.5}Sb_{0.5}$," Appl. Phys. Lett. **44**(7), 677–679 (1984).
[33]M. Cherng, R. Cohen, and G. Stringfellow, "$GaAs_{1-x}Sb_x$ growth by OMVPE," J. Electron. Mater. **13**(5), 799–813 (1984).
[34]M. Pristovsek, M. Zorn, U. Zeimer, and M. Weyers, "Growth of strained GaAsSb layers on GaAs(001) by MOVPE," J. Cryst. Growth **276**(3–4), 347–353 (2005).
[35]D. Wood and A. Zunger, "Epitaxial effects on coherent phase-diagrams of alloys," Phys. Rev. B **40**(6), 4062–4089 (1989).
[36]R. Beanland, M. Aindow, T. Joyce, P. Kidd, M. Lourenco, and P. Goodhew, "A study of surface cross-hatch and misfit dislocation-structure in $In_{0.15}Ga_{0.85}As/GaAs$ grown by chemical beam epitaxy," J. Cryst. Growth **149**(1–2), 1–11(1995).
[37]I. Garcia, R. M. France, J. F. Geisz, and J. Simon, "Thin, high quality GaInP compositionally graded buffer layers grown at high growth rates for metamorphic III-V solar cell applications," J. Cryst. Growth **393**, 64–69 (2014).